

Fabrication of cost effective Pt and FTO-free counter electrode for ZnO based dye sensitized solar cell using thermally decomposed $\text{Cu}_2\text{ZnSnS}_4$ nanoparticles

Chaitanya Bathina¹, Krishnaiah Mokurala^{2*}, Prasanth Ravindran¹, Parag Bhargava², Sudhanshu Mallick^{2*}

¹Center for Green Energy Technology, Pondicherry University, R.V. Nagar, Kalapet, Puducherry - 605 014, India

²Department of Metallurgical Engineering & Materials Science, Indian Institute of Technology Bombay, Maharashtra 400076, India

*Corresponding author. Tel: (+91) 22-25767641; Fax: (+91) 22-25726975; E-mail: krishna887@iitb.ac.in, mallick@iitb.ac.in

Received: 19 October 2015, Revised: 02 February 2016 and Accepted: 26 May 2016

ABSTRACT

Use of Pt and fluorine-doped tin oxide (FTO) substrate together as a counter electrode (CE) significantly increases the fabrication cost of dye-sensitized solar cells (DSSCs). In the present study, we report the cost effective Pt and FTO-free ($\text{Cu}_2\text{ZnSnS}_4$ (CZTS) nanoparticle coated on W substrate) CE for ZnO-based DSSCs. Phase purity, the morphology and elemental composition of synthesized ZnO, CZTS nanoparticles and films were confirmed by physical characteristics such as XRD, FEG-TEM, and FEG-SEM respectively. Cyclic voltammetry study confirmed electrochemical catalytic activity of CZTS films. DSSCs fabricated with CZTS film on W and FTO substrate as CE exhibited efficiencies of 2% and 2.8%, respectively. Conventionally used Pt-based CE demonstrated an efficiency of 3.8 %. Copyright © 2016 VBRI Press.

Keywords: $\text{Cu}_2\text{ZnSnS}_4$; thermal decomposition of metal precursors; tungsten (W); dye-sensitized solar cells, I-V characteristics; counter electrode.

Introduction

Dye-sensitized solar cells (DSSCs) have emerged as promising alternatives to silicon-based photovoltaics because of their easy fabrication process, non-toxic earth abundant constituents and relatively high conversion efficiency [1]. TiO_2 based DSSCs are well explored, and significant research work has been done to improve the efficiency till 13% [2]. In contrast to TiO_2 based DSSCs, ZnO-based DSSCs also have gained considerable importance due to its facial synthesis of ZnO nanoparticles with different morphologies along with its desirable properties such as high mobility of charge carriers and good carrier transport ability [3]. These properties improve the overall efficiency of the ZnO - based DSSCs. The maximum efficiency of 8.03% has been reported for ZnO-based DSSCs with Pt-based counter electrode [4]. Conventionally, Pt coated on the fluorine-doped tin oxide (FTO) substrate is used as a counter electrode (CE) for DSSCs. However, the use of Pt and FTO substrate significantly increases the cost of DSSCs, which in turn affects the commercialization of DSSCs [1-2]. Therefore, it motivated researchers to work on cost effective alternatives to Pt and FTO based CEs. Tungsten (W) deposited on the soda lime glass (SLG) substrate can be utilized as a promising substitute to FTO substrates due to its high conductivity and noncorrosive nature towards the iodide based electrolyte.

Recently, several materials such as a carbon black, mesoporous carbon nanotubes, graphene composites, transition metal sulfides, nitrides, carbides, oxides and earth-abundant quaternary sulfides have been examined as potential candidates to replace Pt-based counter electrode (CE) [5-6]. Apart from these, quaternary sulfides nanoparticles (CZTS, $\text{Cu}_2\text{FeSnS}_4$ (CFTS) and $\text{Cu}_2\text{CoSnS}_4$ (CCTS) have been extensively explored as potential CE material for TiO_2 based DSSCs [6-7]. These materials (CZTS, CFTS, and CCTS) possess electrocatalytic activity similar to that of Pt-based CE [6-7]. However, quaternary sulfides based CEs for ZnO based – DSSCs not yet report in the literature. CZTS nanoparticles have been synthesized via different processes such as solvothermal synthesis [8], hydrothermal synthesis [9], hot injection [10] and thermal decomposition method [11]. Amongst all, thermal decomposition process is a single step method for synthesizing crystalline CZTS nanoparticles in lesser processing time (1h) at a relatively lower temperature [11].

In the present work, we report the synthesis of ZnO nanorods at room temperature via solid state reaction method. CZTS nanoparticles were synthesized by thermal decomposition method. Physical characteristics of the synthesized ZnO and CZTS nanoparticles were carried out. The electrocatalytic activity of CZTS based CEs was compared with that of Pt-based CE. For the first time, fabrication of Pt and FTO-free CE for ZnO-based DSSCs

has been attempted. The performance of DSSCs fabricated with CZTS based CEs was compared with the conventional Pt-based CE.

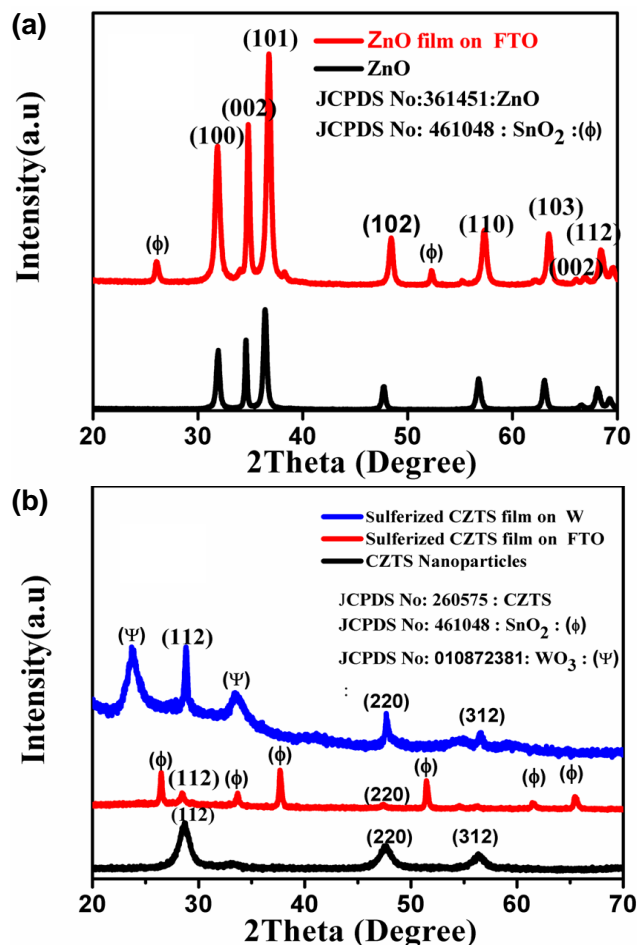


Fig. 1. XRD patterns of (a) synthesized ZnO nanorods at room temperature and film sintered at 400° C for 2 h (b) CZTS nanoparticles synthesized at 300° C for 1 h and CZTS films sulfurized at 525° C for 30 min.

Experimental

Raw materials

The precursors used for the experimental work were: Copper acetate monohydrate ($\text{Cu}(\text{CH}_3\text{COO})_2 \cdot \text{H}_2\text{O}$, SRL, AR Grade), zinc acetate dihydrate ($\text{Zn}(\text{CH}_3\text{COO})_2 \cdot 2\text{H}_2\text{O}$, Thomas Baker, AR grade), tin chloride dihydrate ($\text{SnCl}_2 \cdot 2\text{H}_2\text{O}$, Merck, GR grade), thiourea ($\text{CS}(\text{NH})_2$, SD Fine, AR grade), NaOH (Merck) and ethanol (Merck).

Synthesis of ZnO nanorods and fabrication of ZnO-based photoanode

Solid state synthesis process synthesized ZnO nanorods at room temperature which were subsequently utilized for fabricating photoanode. The following steps were involved in the fabrication of ZnO-based photoanode: 5gm NaOH (Merck) and 7.4 gm of $\text{Zn}(\text{CH}_3\text{COO})_2 \cdot 2\text{H}_2\text{O}$ (Merck) were mixed in an agate mortar for 1 h to get a white paste. The obtained paste was dispersed in 50 ml distilled water and ultrasonicated for 20 min for de-agglomeration. The

prepared precipitate was centrifuged for 15 min and the ultrasonication-centrifugation steps were repeated thrice to remove the impurities. The obtained ZnO powder was then washed with ethanol and dried in an oven. 5 gm of the synthesized ZnO nanorods were mixed with 10 ml water and pot milled for 24 h to get homogenous slurry. The prepared slurry was coated over the FTO substrate ($0.5 \text{ cm} \times 0.5 \text{ cm}$) by doctor blade technique. The film was dried at 80 °C and then sintered at 400 °C for 2 h. This coating-sintering step was repeated several times to obtain a required thickness of about 15-17 μm . Sintered films were taken out at 100 °C and immersed in 0.3 mM ethanol solution of N719 dye (Dyesol, Queanbeyan NSW, Australia) for 24 h at room temperature to proper adsorption.

FTO-free substrate preparation

Tungsten (W) was deposited over SLG substrate with different thicknesses (100 nm, 200 nm, 300 nm, 400 nm, 500 nm) using RF metal sputtering at room temperature (Power = 200W; Working pressure = 2.3×10^{-3} mbar).

Synthesis of nanoparticles and fabrication CZTS based counter electrodes

Detailed synthesis procedure has previously been reported in our paper [11]. To summarize, synthesis process was carried out at 300°C for 1 h in Air atmosphere. Synthesized CZTS nanoparticles were dispersed in toluene and pot milled for 24 h to get homogenous slurry. The obtained slurry was coated on fluorine-doped tin oxide (FTO) substrate and W substrate using drop casting technique. Subsequently, these films were sulfurized at 525 °C for 30 min in Air atmosphere to get the counter electrode for DSSCs.

DSSCs assembly

DSSCs were assembled using the dye loaded ZnO film as photoanode and CZTS coated on FTO /W substrates as CE, respectively. A spacing of approximately 60 μm was maintained between the electrodes using a Surlyn spacer, sandwiched between the electrodes. This gap between the electrodes was filled with an electrolyte composed of : 0.1 M lithium iodide (LiI, Anhydrous, Merck), 0.05M Iodine (I_2 , Thomas Baker, LR), 0.5M 4-tert-Butylpyridine (TBP, Sigma-Aldrich, 96%) and 0.6 M 1-Methyl-3-propylimidazolium iodide (PMII, Sigma-Aldrich, 98%) in acetonitrile.

Characterization of ZnO, CZTS nanoparticle and films and DSSCs

Phase purity of the synthesized ZnO nanoparticles, CZTS nanoparticles, and CZTS films was examined by X-ray diffraction (XRD) technique (PANalytical X-ray diffractometer). XRD was performed in the 2θ scan range of 20° - 80° using $\text{Cu-K}\alpha$ irradiation. Elemental composition of the synthesized ZnO and CZTS nanoparticles were analyzed using energy dispersive spectroscopy (EDS) attached to scanning electron microscope (FEG-SEM, JSM-7600F) being used for

morphological studies. Shape and size of ZnO and CZTS nanoparticles were estimated by field emission gun - transmission electron microscope (FEG-TEM, JEM-7210F). Electrocatalytic activities of the prepared CE were evaluated using cyclic voltammetry. Cyclic voltammetry measurement was carried out using a three-electrode system in an acetonitrile solution (0.1M LiI, 0.05M I₂, and 1M LiClO₄) at a scan rate of 50 mVs⁻¹, ranging from -0.8 to 1.2V. Ag/AgCl was used as the reference electrode, Pt wire as the CE and the prepared CE (0.25 cm²) were used as the working electrodes. Current- Voltage, (I-V) characteristics of the fabricated cells, was measured using a Keithley 2420 source meter (Keithley Instruments, Inc.) under illumination (90 mW/cm²).

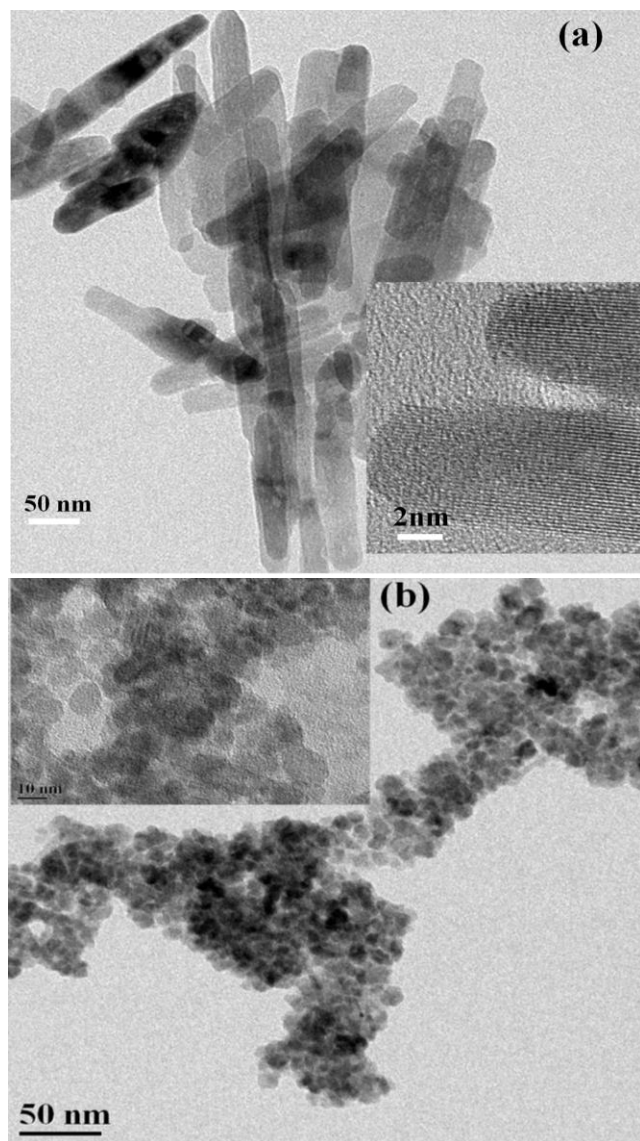


Fig. 2. FEG – TEM images of (a) ZnO nanorods synthesized at room temperature and (b) CZTS nanoparticles synthesized at 300 °C for 1h by thermal decomposition process.

Results and discussion

XRD patterns of synthesized ZnO nanoparticles and sintered film (coated on FTO substrate) are shown in **Fig. 1(a)**. The observed diffraction peaks positioned at

(100), (101), (101), (102), (110), (103) and (112) (**Fig. 1a – black line**) correspond to the single crystalline wurtzite hexagonal phase of ZnO (JCPDS, card no. 36-1451). Similarly, sintered ZnO films show peaks corresponding to wurtzite ZnO (**Fig. 1a – Red line**) along with some additional peaks (Φ) appearing due to the FTO (JCPDF No: 461048) substrate. The XRD patterns of the synthesized nanoparticles and sulfurized CZTS films are shown in **Fig. 1b**. The major diffraction peaks appearing in the XRD patterns (**Fig. 1(b)**) were indexed as CZTS kesterite phase (JCPDS NO: 26-0575). Similarly, sulfurized CZTS films coated on FTO substrate and W substrate show additional peaks (Φ and Ψ) corresponding to the FTO (JCPDS No: 461048) and WO₃ (JCPDS No: 010872381) along with CZTS (**Fig. 1(b)**), respectively.

Field emission gun - transmission electron microscopy (FEG-TEM) reveals that the average length and diameter of the as-prepared ZnO nanorods was approximately 100 nm and 8 nm, respectively (**Fig.2 (a)**). High-resolution TEM (HR-TEM) micrographs show that the ZnO nanoparticles were rod shape and lattice planes being oriented unidirectionally within a single rod (**inset Fig. 2a**). FEG-TEM image of CZTS nanoparticles shows that particles are in an agglomerated form and the size of the agglomerates ranging from 7-14 nm approximately (**Fig. 2b**).

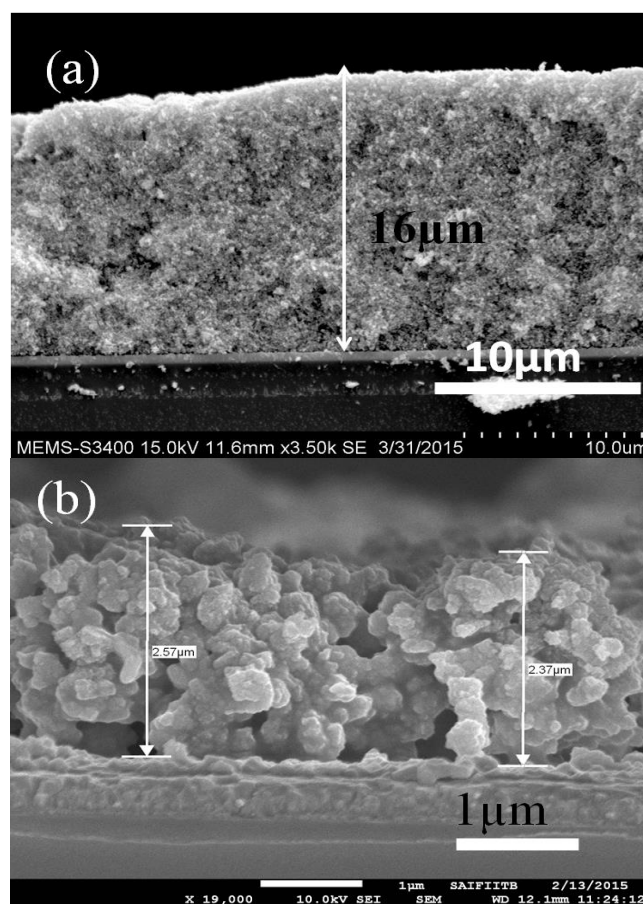


Fig. 3. Cross-sectional micrographs of (a) ZnO sintered film and (b) CZTS film sulfurized at 525 °C for 30 min.

Fig. 3 shows the cross-sectional SEM micrograph of ZnO films. The films are found to be porous as observed in **Fig. 3a**. The thickness of the ZnO film as measured by

surface profilometer was in accordance with the thickness observed through SEM micrograph (Fig. 3a) that was measured to be 16 μm , approximately. Fig. 3b shows the FEG-SEM micrograph for the cross section of the sulfurized CZTS (coated on FTO) film at 525°C for 30 min. The thickness of the CZTS film was observed to be approximately 2.4 μm and further confirmed by a surface profilometer. The elemental composition of sulfurized CZTS film was analyzed by energy dispersive spectroscopy (EDS). The relative elemental ratio of Cu: Zn: Sn: S was estimated to be 2.08: 1.12: 0.96: 3.86.

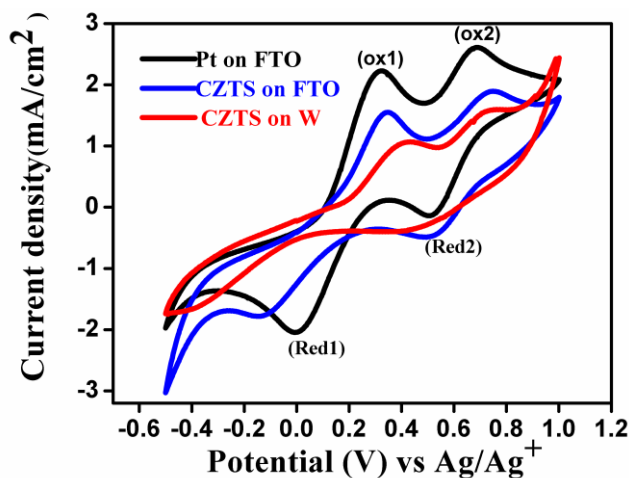


Fig. 4. Cyclic voltammograms for Pt-based CE, CZTS - FTO and W based CEs.

Electrocatalytic activity of the Pt and CZTS coated on FTO and W substrates as CEs respectively was evaluated using cyclic voltammetry. Cyclic voltammetry measurement was carried out using a three-electrode system in an iodide-based ($\text{I}_3^- / \text{I}^-$) electrolyte solution. Cyclic voltammograms (CVs) of Pt and CZTS - FTO based CE show pairs of two redox peaks (Fig. 4). The first pair (ox₁ and red₁) attributes to the redox reaction of $\text{I}_3^- / \text{I}^-$, which is responsible for the regeneration of dye. Whereas, the second pair (ox₂ and red₂) corresponds to the redox reaction of $\text{I}_2 / \text{I}_3^-$. In contrast, the pair of weak redox peaks was observed in the CV plot of the CZTS - W based CE, which attributed to the presence of WO_3 in the CZTS film.

The following equations give information regarding the significance each peak in the CV curve [6, 12].

$$I_{\text{ox1}} : \text{I}^- = \text{I}_3^- + 2\text{e}^-, I_{\text{ox2}} : \text{I}_3^- = \text{I}_2 + 2\text{e}^- \quad (1)$$

$$I_{\text{red1}} : \text{I}_3^- + 2\text{e}^- = \text{I}^-, I_{\text{red2}} : 3\text{I}_2 + 2\text{e}^- = \text{I}_3^- \quad (2)$$

The electrocatalytic activity of different CEs evaluated by cathode current density (I_{Red1}) and peak-to-peak separation (E_{pp}) [6, 12]. The rate constant of a redox reaction is inversely proportional to its peak to peak separation (E_{pp}) value is calculated using the formula [12],

$$E_{\text{pp}} = E_{\text{p}} (\text{anode}) - E_{\text{c}} (\text{Cathode}) \quad (3)$$

The relationship between the cathode current density with diffusion coefficient (D_n) of I_3^- given below equation [12],

$$I_{\text{Red1}} = K (n)^{1.5} A C (D)^{0.5} v^{0.5} \quad (4)$$

where, D is the diffusion coefficient (D) of I_3^- , I_{Red1} is the cathodic current density; K is the constant $= 2.69 \times 10^5$; n means the number of electrodes contributing to the charge transfer (here $n = 2$); A is the area of the CE; C and v represent the concentration of I_3^- species and the scan rate, respectively.

Table 1. Electro catalytic parameters obtained from CV curves.

CEs	I_{Red1} (mA/cm ²)	I_{Ox1} (mA/cm ²)	E_{pp} (meV)
Pt	-2.04	2.25	321
CZTS - FTO	-1.79	1.55	483
CZTS - W	-1.65	1.07	802

From Eq2, the I_{Red1} is proportional to the diffusion coefficient (D) of I_3^- ions which indicates that the higher I_{Red1} , a faster diffusion of I_3^- ions at electrolyte and CE interface. Electrocatalytic parameters obtained from CV curves are summarized in Table 1. From the Table 1, the ascending order of rate of conversion of a redox reaction is Pt ($E_{\text{pp}} = 320$ meV, $I_{\text{Red1}} = -2.04$ mA /cm²) > CZTS - FTO ($E_{\text{pp}} = 483$ meV, $I_{\text{Red1}} = -1.79$ mA /cm²) > CZTS - W ($E_{\text{pp}} = 802$ meV, $I_{\text{Red1}} = -1.65$ mA /cm²).

Table 2. Photovoltaic parameters calculated from the J-V curves.

CEs	V_{oc} (mV)	J_{sc} (mA/cm ²)	FF	η (%)
Pt	631	10.5	0.55	3.8
CZTS - FTO	631	8.4	0.50	2.8
CZTS - W	626	6.3	0.45	2.0

J-V curves for the DSSCs fabricated with CZTS, and Pt-based CEs are shown in Fig. 5. Photovoltaic parameters as calculated from the J-V curves are summarized in Table 2. The DSSCs fabricated with CZTS based CE (coated on FTO) exhibited larger short current density (J_{sc}) (8.40 mA/cm²) as compared to CZTS based CE on W substrate (6.3 mA/cm²). The lower J_{sc} and V_{oc} values of CZTS - W based CE as compared to other CEs is due to higher E_{pp} and lower I_{Red1} and I_{Ox1} values. The obtained Photovoltaic parameters are in good agreement with electrocatalytic parameters (Table 1).

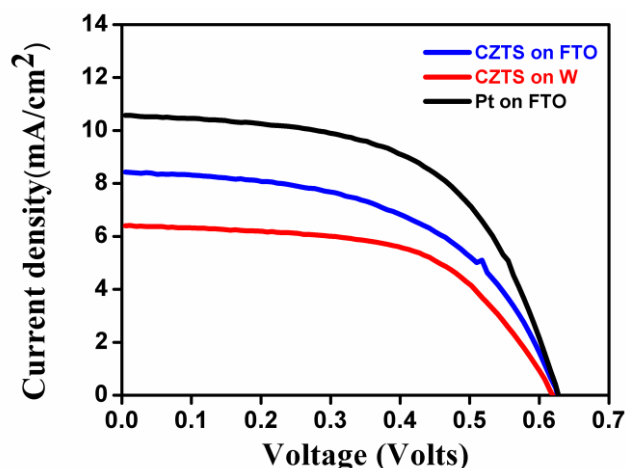


Fig. 5. I-V curves of DSSCs with Pt-based CE, CZTS - FTO and W based CEs.

Conclusions

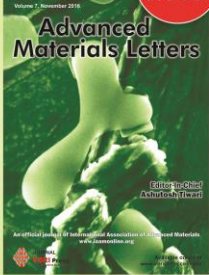
For the first time, Pt and FTO-free (CZTS coated on W substrate) CE were successfully fabricated for ZnO-based dye-sensitized solar cells. FEG – TEM analysis shows that synthesized ZnO nanoparticles were in the form of nanorods while the CZTS particles were observed to be in aggregated form. CZTS based CE was prepared by coating films of the pot milled slurry of CZTS nanoparticles over the FTO and W substrates using an inexpensive drop casting technique. Cyclic voltammetry results demonstrated the CZTS based (coated on FTO) to have a better efficacy to catalyze the reduction of I_3^- to I^- as compared to CZTS based CE (coated on W). DSSCs fabricated with CZTS based CE (coated on FTO, W substrate) exhibited an efficiency of 74%, 53% of the conventionally used Pt-based CE, respectively.

Acknowledgements

The authors would like to acknowledge DST (SERB, SERI program), NCPRE and SERIUS for financial support and SAIF, IIT Bombay for the experimental facilities.

References

1. Regan, B. O.; Grätzel, M., *Nature* **1991**, 353, 737.
DOI: [10.1038/353737a0](https://doi.org/10.1038/353737a0)
2. Mathew, S.; Yella, A.; Gao, P.; Baker, R. H.; Curchod, B. F. E.; Astani, N. A.; Tavernelli, I.; Rothlisberger, U.; Nazeeruddin, Md. K.; Grätzel, M., *Nature Chemistry*, **2014**, 6, 242.
DOI: [10.1038/nchem.1861](https://doi.org/10.1038/nchem.1861)
3. Xu, F.; Sun, L.T., *Energy Environ. Sci.*, **2011**, 4, 818.
DOI: [10.1039/C0EE00448K](https://doi.org/10.1039/C0EE00448K)
4. He, Y.; Hu, J.; Xie, Y., *Chem. Commun.*, **2015**, 51, 16229.
DOI: [10.1039/c5cc04567c](https://doi.org/10.1039/c5cc04567c)
5. Yun, S.; Hagfeldt, A.; Ma, T., *Adv. Mater.*, **2014**, 26, 6210.
DOI: [10.1002/adma.201402056](https://doi.org/10.1002/adma.201402056)
6. Mokurala, K.; Mallick, S.; Bhargava, P., *J. Power Sources*, **2016**, 305, 134.
DOI: [10.1016/j.jpowsour.2015.11.081](https://doi.org/10.1016/j.jpowsour.2015.11.081)
7. Xin, X.; He, M.; Han, W.; Lin, Z., *Angew. Chem. Int. Ed.*, **2011**, 50, 11739.
DOI: [10.1002/anie.201104786](https://doi.org/10.1002/anie.201104786)
8. Zhou, Y. L.; Zhou, W. H.; Li, M.; Du, Y. F.; Wu, S. X., *J. Phys. Chem. C*, **2011**, 115, 19632.
DOI: [10.1021/jp206728b](https://doi.org/10.1021/jp206728b)
9. Liu, W. C.; Guo, B. L.; Wu, X. S.; Zhang, F. M.; Mak, C. L.; Wong, K. H., *J. Mater. Chem. A*, **2013**, 1, 3182.
DOI: [10.1039/C3TA00357D](https://doi.org/10.1039/C3TA00357D)
10. Guo, Q.; Ford, G. M.; Yang, W. C.; Hages, C. J.; Hillhouse, H. W.; Agrawal, R., *Sol. Energy Mater. Sol. Cells.*, **2012**, 105, 132.
DOI: [10.1016/j.solmat.2012.05.039](https://doi.org/10.1016/j.solmat.2012.05.039)
11. Mokurala, K.; Bhargava, P.; Mallick, S., *Mater. Chem. and Phys.*, **2014**, 147, 371.
DOI: [10.1016/j.matchemphys.2014.06.049](https://doi.org/10.1016/j.matchemphys.2014.06.049)
12. Mokurala, K.; Kamble, A.; Bhargava, P.; Mallick, S., *J. Electron. Mater.*, **2015**, 44, 4400.
DOI: [10.1007/s11664-015-3957-4](https://doi.org/10.1007/s11664-015-3957-4)



A Monthly Journal

Advanced Materials Letters

Volume 7, November 2016

Published by VBRI Press

Commitment to Excellence

Publish your article in this journal

Advanced Materials Letters is an official international journal of International Association of Advanced Materials (IAAM, www.iaamonline.org) published monthly by VBRI Press AB from Sweden. The journal is intended to provide high-quality peer-review articles in the fascinating field of materials science and technology particularly in the area of structure, synthesis and processing, characterisation, advanced-state properties and applications of materials. All published articles are indexed in various databases and are available download for free. The manuscript management system is completely electronic and has fast and fair peer-review process. The journal includes review article, research article, notes, letter to editor and short communications.

www.vbripress.com/aml

Copyright © 2016 VBRI Press AB, Sweden